ACS APPLIED MATERIALS & INTERFACES

Research Article

www.acsami.org

Dextran-Gated, Multifunctional Mesoporous Nanoparticle for Glucose-Responsive and Targeted Drug Delivery

Arjyabaran Sinha, Atanu Chakraborty, and Nikhil R. Jana*

Centre for Advanced Materials, Indian Association for the Cultivation of Science, Kolkata-700032, India

Supporting Information

ABSTRACT: Design of drug delivery nanocarrier having targeted recognition followed by bioresponsive controlled release, especially via glucose-responsive release, is a challenging issue. Here, we report magnetic mesoporous silica (MMS)-based drug delivery nanocarrier that can target specific cell and release drug via glucose-responsive gate. The design involves synthesis of MMS functionalized with phenylboronic acid and folate. After drug loading inside the pores of MMS, outside of the pores are closed by dextran via binding with phenylboronic acid. Dextran-gated pores are opened for drug release in the presence of glucose that competes binding with phenylboronic acid. We found that tolbutamide and camptothecin loaded MMS can target beta cells and cancer cells, respectively, release drugs depending on bulk glucose concentration and offers glucose concentration dependent cytotoxicity. Developed functional MMS can be used for advanced drug delivery applications for diabetes and cancers with more efficient therapy.

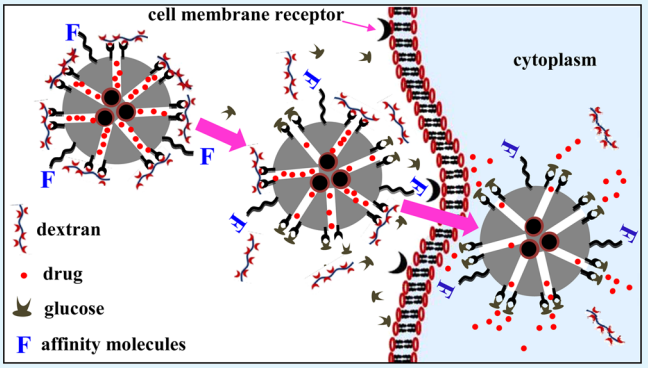

KEYWORDS: *mesoporous silica, responsive drug delivery, bioimaging, cell targeting*

Nanometer size mesoporous silica particles have been extensively used as potential drug delivery carrier.[1−5] They can be synthesized with controlled pores size, incorporated with other nanoparticles, pores and surfaces can be functionalized with desired molecules, and the overall size can be controlled from nanometer to micrometer.[1−5] Compared with traditionally used nanogels and polymer-based drug delivery systems these mesoporous silica are mechanically hard, biocompatible, small in size with option of colloidal form and with high drug loading capacity.[5] Variety of drugs, genes, and proteins are delivered in vitro and in vivo using these mesoporous silica nanocarriers.[1−5] In addition, mesoporous particles have been transformed into advanced drug delivery carrier suitable for controlled and responsive delivery, targeted and controlled delivery, delivery of multiple drugs, and simultaneous delivery and imaging.[1−5]

Common approach for porous material-based controlled drug delivery is to design a gate that can be opened under certain physical/chemical/biological conditions.[3,5] Mesoporous silica has been synthesized with the pore surface capped by nanoparticle,[6] macrocyclic compound,[7] dendrimer,[8] polymer,[9] and biomacromolecule,[10] and the surface of the pores can be opened for drug release in response to different external or internal stimulus. The external stimuli can be temperature,[9] light,[6] magnetic field,[11] or molecules[12] and internal stimuli can be pH,[13] enzyme,[14] reducing agent,[15] or competitive molecule.[16] In addition to that, mesoporous silica has been surface functionalized with folic acid,[17] RGD peptide,[15] antibody,[18] carbohydrate,[19] epidermal growth factor,[20] and aptamer[10] for cell specific targeting/delivery. Nanoparticle incorporated mesoporous silica has been used for simultaneous monitoring and responsive release of drugs.[3,5] Despite the significant progress of the field, successful translation of these drug delivery systems from bench to bedside is limited by complex synthetic design and practical utility of reported stimuli responsive systems.[21]

One important issue is to design carrier material that can target organ/cell and then deliver drug depending on biological requirement.[21] This type of targeted delivery, associated with bioresponsive release, can greatly improve the efficacy of drug performance as it can completely suppress the side effect of drugs. However, design and synthesis of bioresponsive nanocarrier is more challenging as local bioenvironment varies depending on cell/organ. Limited examples of bioresponsive mesoporous silica-based drug delivery carrier include metal-oenzyme responsive gate opening and drug delivery to cancer cell,[22] oligonucleotide responsive gate opening and drug delivery,[10] glucose responsive drug delivery,[12,16,23−26] and other enzyme responsive drug delivery.[14] In particular, glucose responsive drug delivery has great potential in diabetes[27] and cancer treatment.[28] This is because diabetes is associated with high blood sugar along with inefficient insulin production by

Received: August 29, 2014
Accepted: December 2, 2014
Published: December 2, 2014

pancreas and requires the glucose dependent drug targeting to respective cells.[27] Similarly, carbohydrate-based transporters are overexpressed in certain types of cancer cells, and thus, glucose-responsive targeting/delivery may have better therapeutic performance.[28] Thus, attempts have been made to prepare glucose responsive gate in mesoporous silica platform.[12,16,21−26] For example, glucose oxidase-based gate has been used for glucose responsive release of dye,[24] gluconic acid-modified insulin-based gate has been used for glucose responsive release of insulin,[16] and glycoprotein-based gate has been used for glucose responsive release of dye.[25] All these approaches employ protein, enzyme, or functional insulin and thus have very limited practical applications.

Herein, we report mesoporous silica-based multifunctional nanocarrier, which can target and release drug via glucose-responsive gate opening. In addition, a magnetic nanoparticle inside a mesopore can be used for magnetic manipulation and imaging-based tracking of nanocarrier. Compared to earlier approaches where glucose-responsive gates are prepared by protein or enzyme, here a gate is prepared by low cost and stable dextran molecule. Dextran-based gating has two additional advantages. It provides polyethylene glycol like functionalization on particle surface that minimizes nonspecific binding interaction with bioenvironment and specifically target cells having glucose transporter. This nanocarrier target pancreatic beta cells and offers bulk glucose concentration dependent cellular delivery of diabetes type II drug. Folate functionalization of this nanocarrier targets cancer cells having folate receptors and offers glucose-responsive cellular delivery of cancer drug.

EXPERIMENTAL SECTION

Materials and Reagents. [3-(2-Aminoethylamino)propyl] trimethoxysilane (AEAPS), tetraethoxysilane (TEOS), tetramethylamonium hydroxide (25 wt % in methanol, TMAH), folic acid, camptothecin, tolbutamide, and dextran (M_r 6000 and 100000) were all purchased from Sigma−Aldrich and used as received. 3-Carboxyphenylboronic acid and 1-ethyl-3-(3-(dimethylamino)propyl)carbodiimide hydrochloride (EDC) were purchased from TCI Chemicals and used as received. Cetyltrimethylammonium bromide (CTAB) was purchased from Alfa Aesar. *N*-hydroxysuccinimide (NHS) was purchased from Fluka. Ammonia (25 wt %) and succinic anhydride were purchased from Merck.

Preparation of Silica Coated Hydrophilic γ-Fe_2O_3 Nanoparticle. Hydrophobic γ-Fe_2O_3 has been synthesized by reported high temperature thermal degradation method.[29] Next, 1 mL of as synthesized γ-Fe_2O_3 was purified by conventional precipitation-redispersion method and finally dissolved in 10 mL toluene. Next, 5 mL 0.01 M AEAPS and 5 mL 0.01 M TMAH were added to this solution under stirring condition and heated to 70 °C. Heating was continued for 45−60 min, and precipitated particles were successively washed with toluene and ethanol. Finally, solid particles were dissolved in 2 mL water followed by addition of few drops of 0.01 M acetic acid.

Synthesis of Primary Amine Terminated Magnetic Mesoporous Silica Particle (MMS). Primary amine terminated MMS has been synthesized using previously reported method.[30−32] In brief, 2 mL solution of silica coated γ-Fe_2O_3 was mixed with 45 mL distilled water and 5 mL CTAB (0.015 M) solution under the stirring condition. After 15 min, 1.5 mL NH_3 solution (25%) was added. Next, 0.5 mL ethanolic solution of TEOS (300 μL TEOS dissolved in 2.5 mL ethanol), 2 mL ethanolic solution of AEAPS (50 μL AEAPS dissolved in 10 mL ethanol), and 2 mL dimethylformamide were added in a stepwise manner with 5 min intervals, and the whole solution was kept under magnetic stirring condition. After 3 h of reaction, excess ethanol was added to the reaction mixture for particle precipitation. Precipitate was separated from the reaction mixture by centrifugation and washed three times with ethanol and three times with water. Next, particles were dispersed to ethanolic solution of NH_4NO_3 (250 mg NH_4NO_3 dissolved in 25 mL ethanol) by sonication and whole solution was heated to 80 °C for 2 h under stirring condition and the process was repeated twice. This process extracted CTAB present inside the MMS pores. Finally, the particles were dispersed in water and used as stock solution for further use.

Synthesis of Phenylboronic Acid Functionalized MMS (MMS-PBA). MMS-PBA was synthesized from above amine functionalized MMS by EDC-NHS coupling reaction. At first 40 mg of 3-carboxyphenylboronic acid (~0.25 mmol) was dissolved in MES (2-(*N*-morpholino)ethanesulfonic acid) buffer of pH 7.0. Next, 50 mg EDC (~0.25 mmol) and 50 mg NHS (*N*-hydroxysuccinimide) were added to this solution under stirring condition. After 30 min, this solution was mixed with 10 mL of MMS solution and the whole solution was stirred for another 24 h. Next, particles were separated from solution by centrifugation and washed with water and DMF for 4−6 times. Next, particles were dispersed in dry 4 mL DMF, and then, 20 mg succinic anhydride was added and stirring was continued for overnight. Next, particles were separated from solution by high speed centrifugation and washed with DMF for three times for the removal of unreacted reagent. Finally, MMS-PBA particles were dispersed in 10 mL water.

Synthesis of Folic Acid Functionalized MMS-PBA (FA-MMS-PBA). Folate-NHS has been synthesized using our reported method.[33] Next, 2−4 mg of folate-NHS was dissolved in 0.2 mL dimethylfomamide. In a separate vial 10 mL of aqueous solution of phenylboronic acid functionalized MMS was mixed with 1 mL sodium bicarbonate buffer of pH 10. Next, all the folate-NHS solution was added to this solution and whole solution was stirred for another 4−6 h. Finally, particles were collected from solution by centrifugation, washed 5−6 times with bicarbonate buffer solution and dissolved in 5 mL water. This FA-MMS-PBA solution was stored at 4−8 °C for further use.

Preparation of Camptothecin Loaded FA-MMS-PBA and MMS-PBA. About 200 mg of solid FA-MMS-PBA or MMS-PBA particles was suspended in 4 mL DMSO. In a separate vial 10 mg camptothecin was dissolved in 1 mL DMSO and added to particle solution. Stirring was continued for 24 h under dark conditions, and then, particles were separated followed by extensive washing with PBS buffer solution of pH 7.4 to remove any adsorbed camptothecin. Finally, the particles were dispersed in water.

Preparation of Tolbutamide Loaded MMS-PBA. About 200 mg solid MMS-PBA particles were suspended in 4 mL DMSO. In a separate vial 200 mg tolbutamide was dissolved in 2 mL DMSO and mixed with this solution. The stirring was continued for 24 h under dark followed by extensive washing with PBS buffer of pH 7.4 to remove the physisorbed tolbutamide. Finally, the particles were dispersed in 5 mL water.

Preparation of Dextran Functionalized MMS-PBA (MMS-dextran) and FA-MMS-PBA (FA-MMS-dextran). Drug loaded MMS-PBA/FA-MMS-PBA particles were dispersed in PBS buffer of pH 7.4, mixed with 4 mL aqueous solution of dextran (25 mg/mL) and kept under stirring condition for 3 h. Next, particles were separated, washed with PBS buffer of pH 7.4 for the removal of unbound dextrans. Resultant drug loaded MMS-dexran/FA-MMS-dextran was redispersed in aqueous solution for further application.

Measurement of Drug Loading Efficiency. Typically, 5 mg of camptothecin/tolbutamide loaded particles were dispersed in concentrated HCl and then neutralized by NaOH and final volume was maintained to 2 mL. Next, UV−visible spectrum of this solution was measured, and from the calibration curve of camptothecin, we get the concentration of camptothecin. Similarly, we measured the tolbutamide concentration. Typical loading value of camptothecin and tolbutamide was 2−5 μg per mg of material.

Drug Release Study. Drug loaded particles were dispersed in 24 mL PBS buffer solution of pH 7.4 and divided into four parts, each having 8 mL dispersion. Next, 2 mL water or glucose solution was mixed to each vial under the stirring condition such that the final concentration of glucose was 0, 4, 10, and 50 mg/mL. Next, 0.5−1.0 mL of aliquot was collected at different time interval and centrifuged

Scheme 1. Synthesis Strategy for Dextran-Gated Multifunctional Mesoporous Silica Nanocarrier and the Mechanism of Glucose-Responsive Drug Release

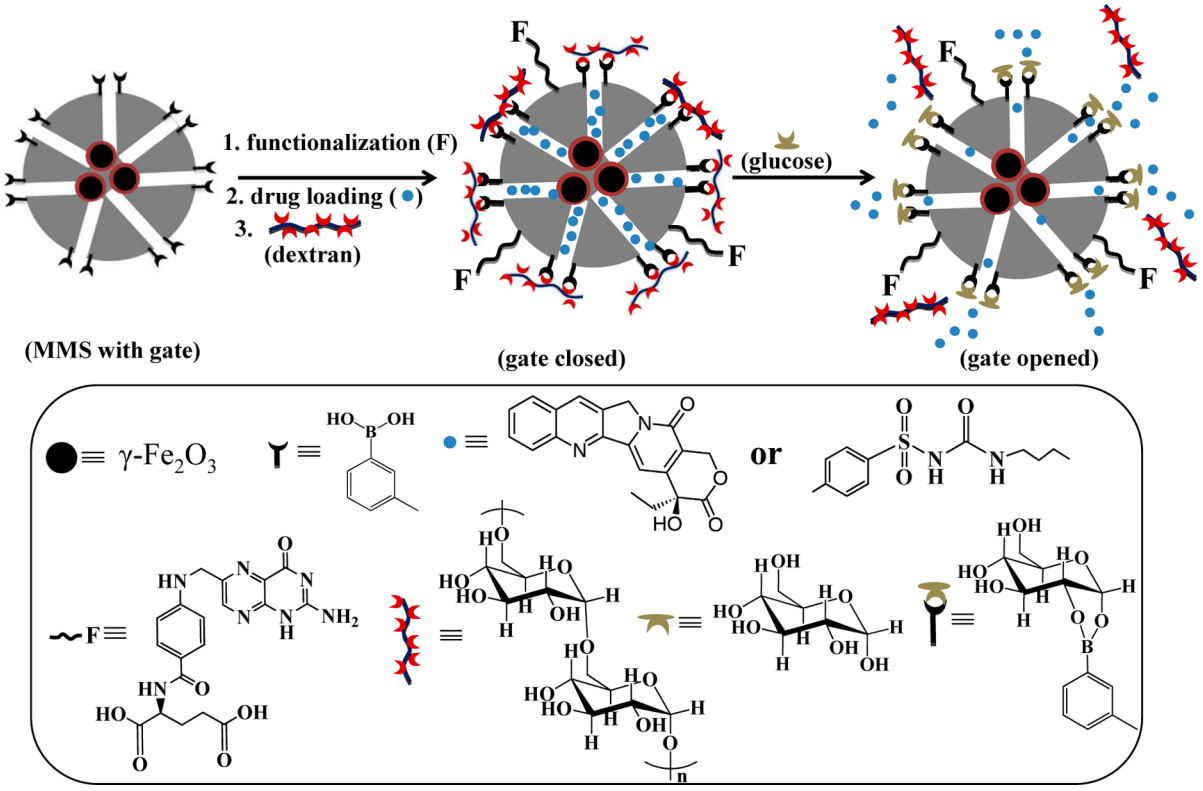

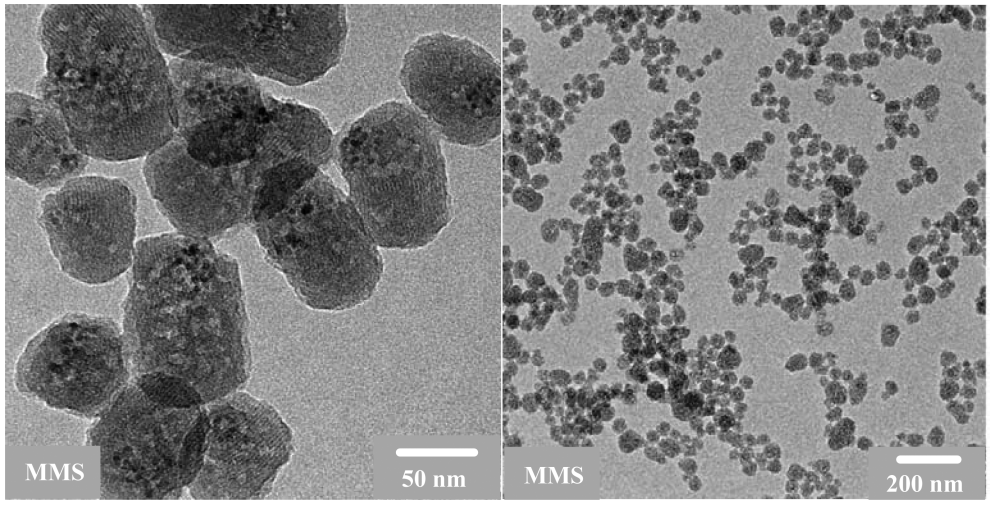

Figure 1. Transmission electron microscopic image of magnetic mesoporous silica nanoparticle (MMS) at high and low magnification.

to separate the particles. The amount of released camptothecin/tolbutamide was monitored by measuring their fluorescence/absorbance in supernatant solution. Camptothecin fluorescence at 450 nm (under 370 nm excitation) and tolbutamide absorbance at 237 nm were used for measurements.

Drug Delivery and Imaging Study. Drug delivery study was performed using HeLa, RIN-5F, and CHO cell lines. Cells were cultured in a tissue culture flask and then subculture in 24 well plates with RPMI culture medium. Next, attached cells along with 0.5 mL RPMI culture medium was mixed with 0.05−0.1 mL drug loaded solution of functional MMS particles (5 mg/mL) and placed in a CO_2 incubator at 37 °C for 1−3 h. Next, cells were washed with PBS buffer of pH 7.4 to remove the unbound particles and mixed with fresh culture medium. Finally, cells were imaged under fluorescence microscope using UV excitation to observe the drug uptake.

Prussian Blue Staining. Functional MMS labeled cells were washed with PBS buffer of pH 7.4 to remove the unbound particles and mixed with 4% paraformaldehyde for 30 min for fixing. After two additional washing with PBS 7.4 buffer, cells were incubated for 1 h with 4% potassium ferrocyanide and 4% HCl solution. Finally, cells were washed with PBS buffer of pH 7.4 and imaged under microscope. Blue color coming from the cells indicates the intracellular delivery of functional MMS.

MTT Assay. Cells were cultured in 24 well plate along with RPMI or glucose free RPMI media and attached cells were incubated with drug loaded functional MMS for 24 h. Next, 50 μL of freshly prepared MTT solution (5 mg/mL) was added to the each well plate and

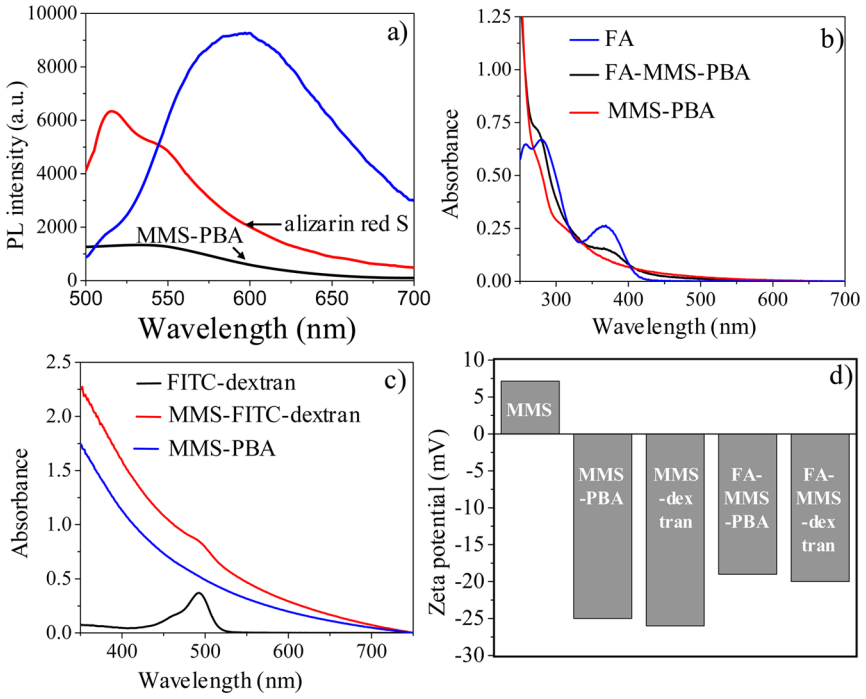

Figure 2. (a) Appearance of red emission after adding alizarin red S to MMS-PBA (blue spectrum). Red and black spectra indicate emission from pure alizarin red S and MMS-PBA, respectively. (b) UV−visible absorption spectra of dispersion of MMS-PBA before and after folate functionalization. Appearance of 370 nm band indicates folate functionalization. (c) UV−visible absorption spectra of MMS-PBA before and after functionalization with FITC-dextran. Characteristic absorption band for FITC at 492 nm suggest the functionalization with dextran. (d) Surface charge of various functional MMS at PBS buffer solution of pH 7.4, as observed via zeta potential measurement.

incubated for another 3 h. Next, supernatant was removed carefully and the violet formazan was dispersed in DMF−water mixture and the absorbance was measure at 570 nm using microplate reader. Cell viability was obtained considering 100% cell viability for the control sample without any materials.

RESULTS AND DISCUSSION

Synthesis and Characterization of Dextran-Gated Magnetic Mesoporous Nanoparticle. Scheme 1 shows the steps involve in synthesis of nanocarrier and the mechanism of glucose-responsive drugs release. Monodisperse iron oxide nanoparticles are synthesized by high temperature thermal degradation methods and transformed into silica coated water-soluble nanoparticle.[29] Next, primary amine terminated magnetic mesoporous silica nanoparticle (MMS) is synthesized in the presence of silica coated iron oxide nanoparticle, using CTAB-based template.[30] Resultant MMS is isolated by centrifugation followed by removal of CTAB. MMS is then functionalized with carboxyphenylboronic acid via EDC coupling and in some cases also functionalized with folate using NHS-folate.[33] Rest of the primary amines are then reacted with succinic anhydride to provide carboxylate functional groups. The functional MMS is then loaded with drug followed by incubation with dextran of molecular weight 100 000. At this stage, polymeric dextran binds with phenylboronate via multiple 1,2-diol groups,[34,35] closes the surface of all pores and thus blocks the drug release. The pores are then opened for drug release via replacement of dextran by glucose having single 1,2-diol group that compete binding with phenylboronic acid.

Structure of typical MMS is shown in Figure 1. As synthesized γ-Fe_2O_3 nanoparticles are of 5−6 nm in size and MMS are of 60−80 nm size (Figure 1 and Supporting Information, Figure S1). The porous structure of MMS and incorporation of γ-Fe_2O_3 nanoparticles inside silica matrix is clearly observed from TEM image. The XRD, surface area measurement, and magnetic measurement study show that as synthesized γ-Fe_2O_3 nanoparticles retain their structure after incorporation into silica matrix[30] (Supporting Information, Figure S2−S5). Nitrogen adsorption/desorption isotherm and corresponding pore size distribution of the MMS show the characteristic type-IV isotherm commonly observed for mesoporous materials with the pore size of 2.1 nm, pore volume of 0.15 cc/g, and surface area in the range from 150 to 300 m^2/g[30−32] (Supporting Information, Figure S3). The surface area and pore volume of drug loaded MMS-dextran becomes 95 m^2/g and 0.05 cc/g, respectively (Supporting Information, Figure S4). Blocking of pores by drug loading and capping of pores by dextran are responsible for such a decrease of surface area and pore volume.

Functionalization of MMS has been characterized at each step via spectroscopic and thermogravimetric analysis. (Figure 2 and Supporting Information, Figure S6−S8) Phenylboronic acid functionalization of MMS (MMS-PBA) has been characterized by alizarin red S test,[36] fluorescence and FTIR study. Alizarin red S reacts with boronic acid giving fluorescence at 590 nm, which is otherwise nonfluorescent. In addition phenylboronic acid itself has fluorescence at 340 nm and similar fluorescence is observed in MMS-PBA (Supporting Information, Figure S6). FTIR study also shows respective vibration signals of phenylboronic acid after functionalization of MMS. (Supporting Information, Figure S7) Similarly, folic acid functionalization of MMS-PBA (FA-MMS-PBA) is confirmed from the appearance of typical absorbance band of folate after functionalization (Figure 2b). Dextan functionalization of MMS-PBA (MMS-dextran) or FA-MMS-PBA (FA-MMS-

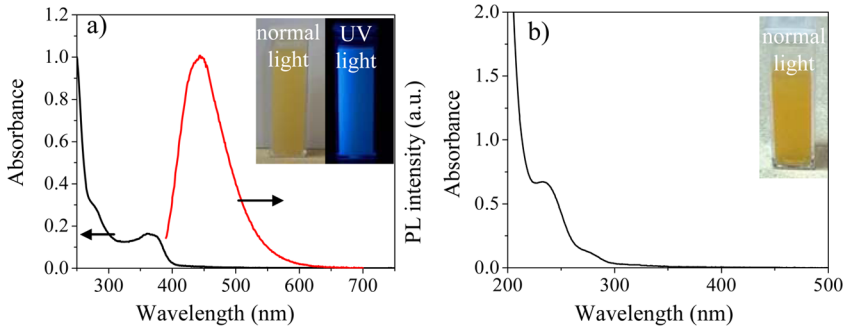

Figure 3. (a) UV−visible and fluorescence spectrum of camptothecin loaded FA-MMS-dextran. Inset shows the digital image of drug loaded colloidal solution under normal and UV light. (b) UV−visible spectrum of tolbutamide loaded MMS-dextran. Inset shows the digital image of drug loaded colloidal solution under normal light.

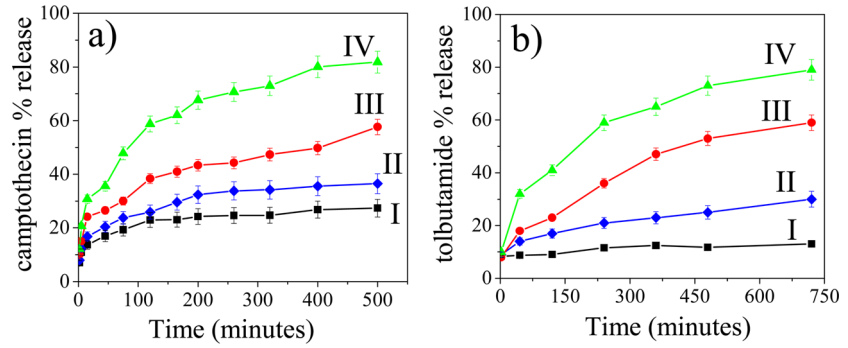

Figure 4. (a) Glucose-responsive release of camptothecin from camptothecin loaded colloidal FA-MMS-dextran at pH 7.4, under different concentration of glucose. (b) Glucose-responsive release of tolbutamide from tolbutamide loaded MMS-dextran at pH 7.4, under different concentration of glucose. [I, 0 mg/mL; II, 4 mg/mL; III, 10 mg/mL; IV, 50 mg/mL].

dextran) via formation of cyclic ester between 1,2-cis diol of dextran and boronate group has been confirmed using a control experiment with FITC-dextran. Incubation of FITC-dextran with MMS-PBA, followed by extensive washing/separation of unreacted FITC-dextran, still shows the absorption band of FITC suggesting that FITC is attached with MMS-PBA. This result suggests that dextran is covalently attached with MMS-PBA (Figure 2c). Dynamic light scattering study shows that average hydrodynamic size of the most of the functional MMS varies between 100 and 160 nm but increased significantly to 190 nm after dextran functionalization. This size increase is expected considering the fact that dextran provide extended layer around particle surface. Zeta potential measurement shows that MMS changes it surface charge from positive to negative after converting into MMS-PBA and remain negative after functionalization with folate, carboxylate, and dextran (Figure 2d). The amounts of phenylboronic acid and dextran attached to the MMS have been estimated from thermogravimetric analysis (Supporting Information, Figure S8). It shows that ∼2.5 wt % of phenylboronic acid is present in MMS-PBA and ∼7 wt % dextran is present in MMS-dextran. We have also performed TEM study to observe the dextran coating in MMS-dextran. We found that dextran layer around MMS is hard to visualize due to poor contrast and in addition the porous structure of silica becomes invisible after dextran coating (Supporting Information, Figure S9). We presume that presence of dextran makes this effect and may be an indirect evidence of dextran capping.

Glucose-Responsive Drug Release. Drug loading can be performed by simple incubation of MMS-PBA/FA-MMS-PBA with drug solution followed by separation of free drug and finally incubation with dextran solution to close the pore surface. This results formation of dextran coated MMS-PBA (MMS-dextran) and dextran coated FA-MMS-PBA (FA-MMS-dextran) with loaded drug. We have selected two drugs namely camptothecin and tolbutamide as representative of anticancer and diabetes type II drugs, respectively. Figure 3 shows the colloidal solution of camptothecin loaded FA-MMS-dextran and tolbutamide loaded MMS-dextran. Results show that MMS retains colloidal stability after drug loading and in addition associated with the optical property of drug. For example, camptothecin loaded MMS shows typical absorption and blue emission of camptothecin and tolbutamide loaded MMS shows the absorption property of tolbutamide.

Glucose-responsive release of drug from drug loaded MMS-dextran/FA-MMS-dextran is shown in Figure 4. Glucose has one 1,2 cis diol that competes binding with phenylboronic acid and thus removes the larger size dextran from the pore surface. This processes of pore opening leads to the release of drugs from inside MMS to the bulk solution. Result of release profile of camptothecin and tolbutamide is shown in Figure 4. It shows that in absence of glucose camptothecin/tolbutamide release in 6−12 h time is only 10−20%, indicating that dextran has capped the pores efficiently and has blocked the drug release. In contrast, when glucose is present in bulk solution, the rate of drug release is significantly enhanced. In addition the drug release rate increases with the increasing glucose concentration. This result indicates that glucose can successfully open the pore surface by replacing dextran and offers the drug release.

Targeted and Glucose-Responsive Cellular Delivery of Drug. Targeted cellular delivery of drug has been performed using drug loaded MMS-dextran and FA-MMS-dextran.

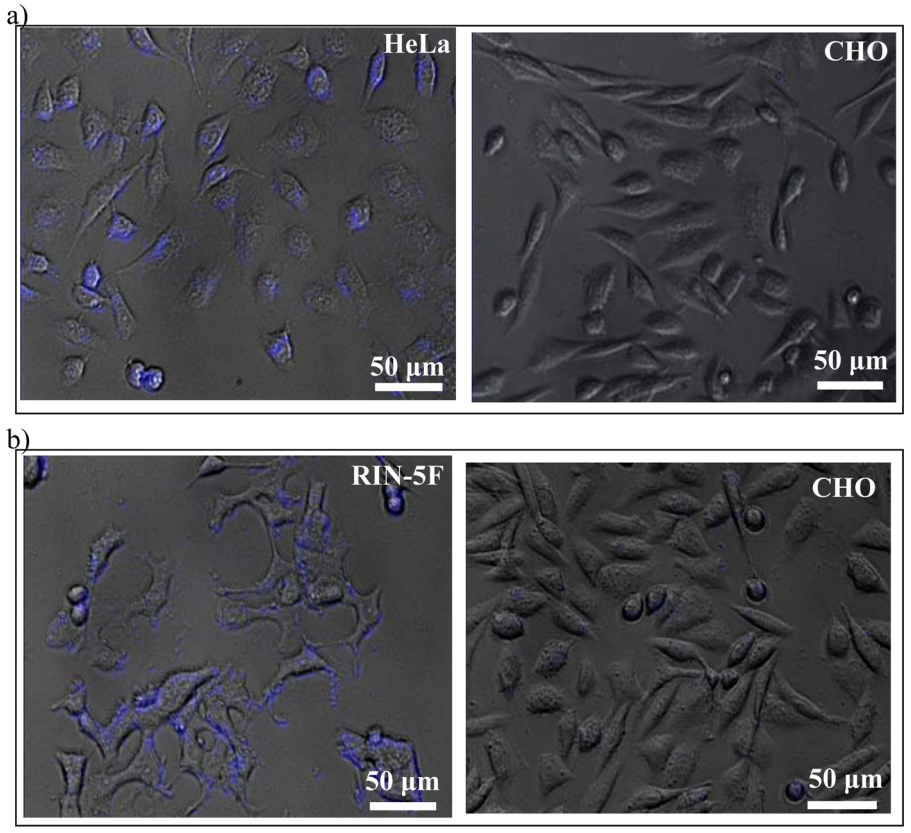

Figure 5. (a) Evidence of targeted cellular delivery of camptothecin using FA-MMS-dextran. HeLa or CHO cells are incubated with camptothecin loaded FA-MMS-dextran for 1 h, and then, bright field and fluorescence images of cells are collected and merged. Blue fluorescence of camptothecin inside cells indicates that it has been delivered to HeLa cells but not to CHO cells. (b) Evidence of targeted cellular delivery of camptothecin using MMS-dextran. RIN-5F or CHO cells are incubated with camptothecin loaded MMS-dextran for 3 h, and then, bright field and fluorescence images of cells are collected and merged. Blue fluorescence of camptothecin inside cells indicates that it has been delivered to RIN-5F cells but not to CHO cells.

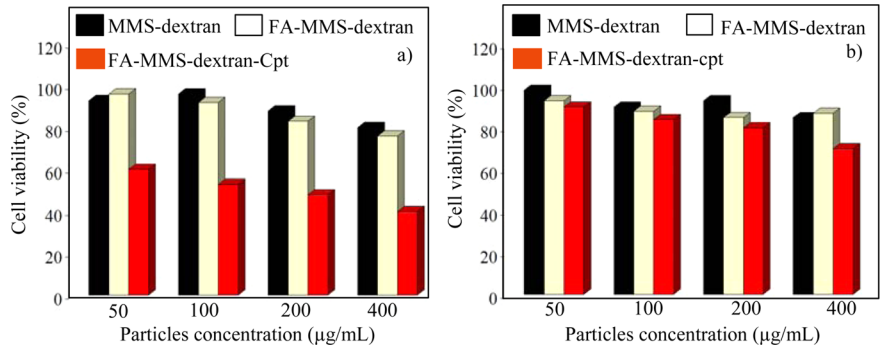

Figure 6. Cytotoxicity of camptothecin loaded FA-MMS-dextran (FA-MMS-dextran-cpt) toward HeLa cells after 24 h incubation in the presence of conventional cell culture media with glucose (a) and in glucose-free cell culture media (b), showing that drug loaded particle offers bulk glucose concentration dependent cell viability.

Different cell lines have been used for this study that includes HeLa cell with overexpressed folate receptors, RIN-5F cell with overexpressed glucose transporter and CHO cell as control cell. The fluorescence property of camptothecin has been used to monitor the cellular delivery of this drug. The cell culture media used in these studies have glucose concentration of 2−4 mg/mL and thus, glucose-responsive drug release occurs as shown in Figure 4. In some control experiments, glucose-free media has also been used. Results show that FA-MMS-dextran selectively delivers camptothecin to HeLa cells having overexpressed folate receptor but not to CHO cell that does not overexpress folate receptor (Figure 5). Iron oxide present in MMS can be used to visualize the localization of the MMS via Prussian blue test of labeled cells. It is clearly observed that HeLa cells gives positive Prussian blue test as compared to CHO cells, suggesting that MMS specifically label the HeLa cells prior to deliver camptothecin (Supporting Information, Figure S10). Similarly, MMS-dextran can selectively deliver camptothecin to RIN-5F cells, as observed from intense blue emission of camptothecin from cell (Figure 5). However, it cannot deliver camptothecin to CHO cells that do not have glucose transporter. We have also performed imaging study

using fluorescein loaded MMS-dextran and observed the green emission of fluorescein from cell, suggesting delivery of fluorescein to RIN-5F cells (Supporting Information, Figure S11). Similar type of delivery study of tolbutamide is performed with RIN-5F cells but imaging of tolbutamide is not performed as it does not have visible fluorescence.

Impact of these drug delivery carriers toward cytotoxicity has been estimated via MTT assay by incubating the drug loaded MMS with cells for 24 h (Figure 6). The cytotoxicity of camptothecin loaded FA-MMS-dextran toward HeLa cells has been tested and compared with MMS-dextran and FA-MMS-dextran. The results show that cells maintained >75% viability even at highest tested concentration of 400 μg/mL for different functional MMS but in case of camptothecin loaded FA-MMS-dextran the cell viability decreases up to 40%. We have also performed the similar cytotoxicity study in glucose-free medium, which shows >70% cell viability. This result clearly indicates that camptothecin loaded FA-MMS-dextran induces cytotoxicity in the presence of glucose but does not induce cytotoxicity in absence of glucose. This result also indicates that functional MMS has no significant cytotoxic effect on the cell and can be used as drug delivery vehicle to induce cellular toxicity. Similarly, RIN-5F cells are incubated with tolbutamide loaded MMS-dextran and drug-free MMS-dextran for 24 h to investigate the cytoxicity (Supporting Information, Figure S12). Result shows that cells maintain >85% viability in both cases. This result is reasonable considering the fact that tolbutamide is known to activate pancreatic β-cells for enhanced insulin secretion without significant toxicity.[37,38] This result indicates that MMS-dextran with tolbutamide is nontoxic toward the pancreatic β-cells and can be used as safe drug delivery carrier for enhanced insulin secretion.[37,38]

Application Potential of Dextran-Gated Drug Delivery Carrier. We have tested dextran-based capping of pores using two different dextran of molecular weight of 6000 and 100 000 Da. We found that drug release is relatively rapid for low molecular weight dextran and less dependent on bulk glucose concentration. Thus, we have preferred using dextran of molecular weight of 100 000 Da. The better performance for high molecular weight dextran is due to its larger hydrodynamic diameter that acts as good pore blocking agent than lower molecular weight dextran. Targeted delivery and glucose-responsive drug release are two important aspects of presented MMS-based drug delivery. Offered designs have cell targeting property as MMS-dextran can target cells having glucose transporters and FA-MMS-dextran can target cells having overexpressed folate receptors. Glucose-responsive drug release property of MMS-dextran has been demonstrated from bulk glucose concentration dependent drug release to respective cells followed by enhanced cytotoxicity. In addition to that, magnetic nanoparticle present inside MMS can be used for magnetic manipulation, magnetic-based hyperthermia application and imaging-based monitoring of MMS localization.[1−5]

Designed materials can be used for advanced drug delivery applications in diabetic and cancer related application where targeted and glucose-responsive drug delivery may provide more powerful therapeutic effect.[39−44] Diabetes is associated with high blood sugar and inability of pancreas to produce insulin, and it requires the targeting to respective cells followed by drug delivery depending on the level of blood glucose.[40−42] In addition, carbohydrate-based transporters are overexpressed in certain types of cancer cells and thus targeting followed by glucose-responsive delivery may have better therapeutic performance.[43−45] Although several glucose-responsive drug delivery approaches have been developed, they are involved with unstable enzyme or protein-based gating, which have limited practical applications. In contrast, our approach used dextran-based gating that is much more stable, cost-effective, and simple.

CONCLUSIONS

In conclusion, we have synthesized dextran-gated mesoporous silica colloid, which can load drug, target specific cells, and deliver drug depending on bulk glucose concentration. The design involves synthesis of mesoporous silica functionalized with phenylboronic acid so that pore surface can be capped with dextran via the binding of 1,2-diol groups with phenylboronic acid. The pore of phenylboronic acid functionalized particles can be loaded with drugs followed by dextran-based closing of pore surface, and then, pores can be opened for drug release by glucose that competes for binding with phenylboronic acid. Particles can be further functionalized with other affinity molecules for specific targeting. It is shown that dextran-gated particles can target pancreatic beta cells and offers glucose-responsive delivery of diabetic drug tolbutamide. Similarly, dextran-gated and folate functionalized particles can target specific cancer cells and offer glucose-responsive drug delivery and toxicity. Developed strategy can be used for advanced drug delivery applications for diabetes/cancers with more efficient therapy.

ASSOCIATED CONTENT

Supporting Information

Details of characterization of mesoporous materials, characterization of functionalization, Prussian blue staining image of particle labeled cells, and cytotoxicity study of RIN-5F cells with drug loaded particle. This material is available free of charge via Internet at http://pubs.acs.org.

AUTHOR INFORMATION

Corresponding Author

*Telephone: +91-33-24734971. Fax: +91-33-24732805. E-mail: camnrj@iacs.res.in.

Notes

The authors declare no competing financial interest.

ACKNOWLEDGMENTS

The authors thank DST, DBT, and CSIR, government of India for financial assistance. A.S. and A.C. acknowledge CSIR, India, for providing research fellowship.

REFERENCES

(1) Vivero-Escoto, J. L.; Slowing, I. I.; Trewyn, B. G.; Lin, V. S.-Y. Mesoporous Silica Nanoparticles for Intracellular Controlled Drug Delivery. *Small* **2010**, *6*, 1952−1967.

(2) Lee, J. E.; Lee, N.; Kim, T.; Kim, J.; Hyeon, T. Multifunctional Mesoporous Silica Nanocomposite Nanoparticles for Theranostic Applications. *Acc. Chem. Res.* **2011**, *44*, 893−902.

(3) Yang, P.; Gai, S.; Lin, J. Functionalized Mesoporous Silica Materials for Controlled Drug Delivery. *Chem. Soc. Rev.* **2012**, *41*, 3679−3698.

(4) Wang, K.; He, X.; Yang, X. H.; Shi, H. Functionalized Silica Nanoparticles: A Platform for Fluorescence Imaging at the Cell and Small Animal Levels. *Acc. Chem. Res.* **2013**, *46*, 1367−1376.

(5) Argyo, C.; Weiss, V.; Brauchle, C.; Bein, T. Multifunctional Mesoporous Silica Nanoparticles as a Universal Platform for Drug Delivery. *Chem. Mater.* **2014**, *26*, 435−451.
(6) Vivero-Escoto, J. L.; Slowing, I. I.; Wu, C. W.; Lin, V. S.-Y. Photoinduced Intracellular Controlled Release Drug Delivery in Human Cells by Gold-Capped Mesoporous Silica Nanosphere. *J. Am. Chem. Soc.* **2009**, *131*, 3462−3463.
(7) Kim, H.; Kim, S.; Park, C.; Lee, H.; Park, H. J.; Kim, C. Glutathione-Induced Intracellular Release of Guests from Mesoporous Silica Nanocontainers with Cyclodextrin Gatekeepers. *Adv. Mater.* **2010**, *22*, 4280−4283.
(8) Gruenhagen, J. A.; Lai, C. Y.; Radu, D. R.; Lin, V. S.-Y.; Yeung, E. S. Real-Time Imaging of Tunable Adenosine 5-Triphosphate Release from an MCM-41-Type Mesoporous Silica Nanosphere-Based Delivery System. *Appl. Spectrosc.* **2005**, *59*, 424−431.
(9) You, Y. Z.; Kalebaila, K. K.; Brock, S. L.; Oupicky, D. Temperature-Controlled Uptake and Release in PNIPAM-Modified Porous Silica Nanoparticles. *Chem. Mater.* **2008**, *20*, 3354−3359.
(10) Zhang, P.; Cheng, F.; Zhou, R.; Cao, J.; Li, J.; Burda, C.; Min, Q.; Zhu, J. J. DNA-Hybrid-Gated Multifunctional Mesoporous Silica Nanocarriers for Dual-Targeted and MicroRNA-Responsive Controlled Drug Delivery. *Angew. Chem., Int. Ed.* **2014**, *53*, 2371−2375.
(11) Chen, P. J.; Hu, S. H.; Hsiao, C. S.; Chen, Y. Y.; Liu, D. M.; Chen, S. Y. Multifunctional Magnetically Removable Nanogated Lids of Fe_3O_4-Capped Mesoporous Silica Nanoparticles for Intracellular Controlled Release and MR Imaging. *J. Mater. Chem.* **2011**, *21*, 2535−2543.
(12) Aznar, E.; Villalonga, R.; Gimenez, C.; Sancenon, F.; Marcos, M. D.; Martinez-Manez, R.; Diez, P.; Pingarron, J. M.; Amoros, P. Glucose-Triggered Release Using Enzyme-Gated Mesoporous Silica Nanoparticles. *Chem. Commun.* **2013**, *49*, 6391−6393.
(13) Muharnmad, F.; Guo, M. Y.; Qi, W. X.; Sun, F. X.; Wang, A. F.; Guo, Y. J.; Zhu, G. S. pH-Triggered Controlled Drug Release from Mesoporous Silica Nanoparticles via Intracelluar Dissolution of ZnO Nanolids. *J. Am. Chem. Soc.* **2011**, *133*, 8778−8781.
(14) Bernardos, A.; Mondragon, L.; Aznar, E.; Marcos, M. D.; Martinez-Manez, R.; Sancenon, E.; Soto, J.; Barat, J. M.; Perez-Paya, E.; Guillem, C.; Amoros, P. Enzyme-Responsive Intracellular Controlled Release Using Nanometric Silica Mesoporous Supports Capped with "Saccharides. *ACS Nano* **2010**, *4*, 6353−6368.
(15) Xiao, D.; Jia, H. Z.; Zhang, J.; Liu, C. W.; Zhuo, R. X.; Zhang, X. Z. A Dual-Responsive Mesoporous Silica Nanoparticle for Tumor-Triggered Targeting Drug Delivery. *Small* **2014**, *10*, 591−598.
(16) Zhao, Y.; Trewyn, B. G.; Slowing, I. I.; Lin, V. S. Y. Mesoporous Silica Nanoparticle-Based Double Drug Delivery System for Glucose-Responsive Controlled Release of Insulin and Cyclic AMP. *J. Am. Chem. Soc.* **2009**, *131*, 8398−8400.
(17) Wu, H. X.; Liu, G.; Zhang, S. J.; Shi, J. L.; Zhang, L. X.; Chen, Y.; Chen, F.; Chen, H. R. Biocompatibility, MR Imaging and Targeted Drug Delivery of a Rattle-Type Magnetic Mesoporous Silica Nanosphere System Conjugated With PEG and Cancer-Cell-Specific Ligands. *J. Mater. Chem.* **2011**, *21*, 3037−3045.
(18) Cheng, K.; Blumen, S. R.; MacPherson, M. B.; Steinbacher, J. L.; Mossman, B. T.; Landry, C. C. Enhanced Uptake of Porous Silica Microparticles by Bifunctional Surface Modification with a Targeting Antibody and a Biocompatible Polymer. *ACS Appl. Mater. Interfaces* **2010**, *2*, 2489−2495.
(19) Brevet, D.; Gary-Bobo, M.; Raehm, L.; Richeter, S.; Hocine, O.; Amro, K.; Loock, B.; Couleaud, P.; Frochot, C.; Morere, A.; Maillard, P.; Garcia, M.; Durand, J. O. Mannose-Targeted Mesoporous Silica Nanoparticles for Photodynamic Therapy. *Chem. Commun.* **2009**, 1475−1477.
(20) Mackowiak, S. A.; Schmidt, A.; Weiss, V.; Argyo, C.; von Schirnding, C.; Bein, T.; Brauchle, C. Targeted Drug Delivery in Cancer Cells with Red-Light Photoactivated Mesoporous Silica Nanoparticles. *Nano Lett.* **2013**, *13*, 2576−2683.
(21) Mura, S.; Nicolas, J.; Couvreur, P. Stimuli-Responsive Nanocarriers for Drug Delivery. *Nat. Mater.* **2013**, *12*, 991−1003.
(22) Singh, N.; Karambelkar, A.; Gu, L.; Lin, K.; Miller, J. S.; Chen, C. S.; Sailor, M. J.; Bhatia, S. N. Bioresponsive Mesoporous Silica Nanoparticles for Triggered Drug Release. *J. Am. Chem. Soc.* **2011**, *133*, 19582−19585.
(23) Zhao, W.; Zhang, H.; He, Q.; Li, Y.; Gu, J.; Li, L.; Shi, J. A Glucose-Responsive Controlled Release of Insulin System Based on Enzyme Multilayers-Coated Mesoporous Silica Particles. *Chem. Commun.* . **2011**, *47*, 9459−9461.
(24) Chen, M.; Huang, C.; He, C.; Zhu, W.; Xu, Y.; Lu, Y. Glucose-Responsive Controlled Release System Using Glucose Oxidase-Gated Mesoporous Silica Nanocontainers. *Chem. Commun.* **2012**, *48*, 9522−9524.
(25) Wu, S.; Huang, X.; Du, X. Glucose- and pH-Responsive Controlled Release of Cargo from Protein-Gated Carbohydrate-Functionalized Mesoporous Silica Nanocontainers. *Angew. Chem. Int. Ed.* **2013**, *52*, 5580−5584.
(26) Diez, P.; Sanchez, A.; Gamella, M.; Martinez-Ruiz, P.; Aznar, E.; de la Torre, C.; Murguia, J. R.; Martinez-Manez, R.; Villalonga, R.; Pingarron, J. M. Toward the Design of Smart Delivery Systems Controlled by Integrated Enzyme-Based Biocomputing Ensembles. *J. Am. Chem. Soc.* **2014**, *136*, 9116−9123.
(27) Thorens, B.; Weir, G. C.; Leahy, J. L.; Lodish, H. F.; Weir, S. B. Reduced Expression of the Liver/Beta-Cell Glucose Transporter Isoform in Glucose-Insensitive Pancreatic Beta Cells of Diabetic Rats. *Proc. Natl. Acad. Sci. U.S.A.* **1990**, *87*, 6492−6496.
(28) Xu, C. X.; Zhu, H. H.; Zhu, Y. M. Diabetes and Cancer: Associations, Mechanisms, and Implications for Medical Practice. *World J. Diabetes* **2014**, *5*, 372−380.
(29) Jana, N. R.; Earhart, C.; Ying, J. Y. Synthesis of Water-Soluble and Functionalized Nanoparticles by Silica Coating. *Chem. Mater.* **2007**, *19*, 5074−5082.
(30) Sinha, A.; Jana, N. R. Nanoparticle-Incorporated Functional Mesoporous Silica Colloid for Diverse Applications. *Eur. J. Inorg. Chem.* **2012**, 4470−4478.
(31) Hu, J.; Shaojie Huang, S.; Huang, X.; Kang, Z.; Gan, N. Superficially Mesoporous Fe_3O_4 @SiO_2 Core Shell Microspheres: Controlled Syntheses and Attempts in Protein Separations. *Microporous Mesoporous Mater.* **2014**, *197*, 180−184.
(32) Cheng, G.; Wang, Y.; Wang, Z. G.; Sui, X. J.; Zhang, J. L. Magnetic Mesoporous Silica Incorporated with TiO_2 for Selective and Rapid Capture of Peptides. *RSC Adv.* **2014**, *4*, 7694−7702.
(33) Maity, A. R.; Saha, A.; Roy, A.; Jana, N. R. Folic Acid Functionalized Nanoprobes for Fluorescence-, Dark-Field-, and Dual-Imaging-Based Selective Detection of Cancer Cells and Tissue. *Chem. Plus. Chem.* **2013**, *78*, 259−267.
(34) Wu, X.; Li, Z.; Chen, X. X.; Fossey, J. S.; James, T. D.; Jiang, Y. B. Selective Sensing of Saccharides Using Simple Boronic Acids and Their Aggregates. *Chem. Soc. Rev.* **2013**, *42*, 8032−8048.
(35) Zhang, L. Z.; Lin, Y.; Wang, J. J.; Yao, W.; Wu, W.; Jiang, X. Q. A Facile Strategy for Constructing Boron-Rich Polymer Nanoparticles via a Boronic Acid-Related Reaction. *Macromol. Rapid Commun.* **2011**, *32*, 534−539.
(36) Springsteen, G.; Wang, B. Alizarin Red S. as a General Optical Reporter for Studying the Binding of Boronic Acids with Carbohydrates. *Chem. Commun.* **2001**, 1608−1609.
(37) Koster, J. C.; Permutt, M. A.; Nichols, C. G. Diabetes and Insulin Secretion—The ATP-Sensitive K^+ Channel (K_{ATP}) Connection. *Diabetes* **2005**, *54*, 3065−3072.
(38) Pfeifer, M. A.; Halter, J. B.; Porte, D. Insulin-Secretion in Diabetes-Mellitus. *Am. J. Med.* **1981**, *70*, 579−588.
(39) Subramani, K. Applications of Nanotechnology in Drug Delivery Systems for the Treatment of Cancer and Diabetes. *Int. J. Nanotechnol.* **2006**, *3*, 557−580.
(40) Bratlie, K. M.; York, R. L.; Invernale, M. A.; Langer, R.; Anderson, D. G. Materials for Diabetes Therapeutics. *Adv. Healthcare Mater.* **2012**, *1*, 267−284.
(41) Ravaine, V.; Ancla, C.; Catargi, B. Chemically Controlled Closed-Loop Insulin Delivery. *J. Controlled Release* **2008**, *132*, 2−11.

(42) Fajans, S. S.; Brown, M. B. Administration of Sulfonylureas Can Increase Glucose-Induced Insulin Secretion for Decades in Patients with Maturity-Onset Diabetes off the Young. *Diabetes Care* **1993**, *16*, 1254−1261.
(43) Lamkin, D. M.; Spitz, D. R.; Shahzad, M. M. K.; Zimmerman, B.; Lenihan, D. J.; DeGeest, K.; Lubaroff, D. M.; Shinn, E. H.; Sood, A. K.; Lutgendorf, S. K. Glucose as a Prognostic Factor in Ovarian Carcinoma. *Cancer* **2009**, *115*, 1021−1027.
(44) Krzeslak, A.; Wojcik-Krowiranda, K.; Forma, E.; Jozwiak, P.; Romanowicz, H.; Bienkiewicz, A.; Brys, M. Expression of GLUT1 and GLUT3 Glucose Transporters in Endometrial and Breast Cancers. *Pathol. Oncol. Res.* **2012**, *18*, 721−728.
(45) Gatenby, R. A.; Gillies, R. J. Why do Cancers have High Aerobic Glycolysis? *Nat. Rev. Cancer* **2004**, *4*, 891−899.